

Geophysical Research Letters

RESEARCH LETTER

10.1029/2019GL083719

Key Points:

- Tropical cyclones enhance labile carbon export to the deep oligotrophic ocean
- Lipid fluxes to the deep ocean may increase more than 1 order of magnitude after hurricane passage
- Climate-induced changes in hurricane activity may impact deep ocean ecosystems and elemental cycling

Supporting Information:

- Supporting Information S1

Correspondence to:

R. Pedrosa-Pàmies,
rpedrosa@mbl.edu

Citation:

Pedrosa-Pàmies, R., Conte, M. H., Weber, J. C., & Johnson, R. (2019). Hurricanes enhance labile carbon export to the deep ocean. *Geophysical Research Letters*, *46*, 10,484–10,494. <https://doi.org/10.1029/2019GL083719>


Received 15 MAY 2019

Accepted 13 AUG 2019

Accepted article online 16 AUG 2019

Published online 7 SEP 2019

Hurricanes Enhance Labile Carbon Export to the Deep Ocean

R. Pedrosa-Pàmies¹ , M. H. Conte^{1,2} , J. C. Weber¹, and R. Johnson² 

¹The Ecosystems Center, Marine Biological Laboratory, Woods Hole, MA, USA, ²Bermuda Institute of Ocean Science, St. Georges GE01, Bermuda

Abstract Tropical cyclones (hurricanes) generate intense surface ocean cooling and vertical mixing resulting in nutrient upwelling into the photic zone and episodic phytoplankton blooms. However, their influence on the deep ocean remains unknown. Here we present evidence that hurricanes also impact the ocean's biological pump by enhancing export of labile organic material to the deep ocean. In October 2016, Category 3 Hurricane Nicole passed over the Bermuda Time Series site in the oligotrophic NW Atlantic Ocean. Following Nicole's passage, particulate fluxes of lipids diagnostic of fresh phytodetritus, zooplankton, and microbial biomass increased by 30–300% at 1,500 m depth and 30–800% at 3,200 m depth. Mesopelagic suspended particles following Nicole were also enriched in phytodetrital material and in zooplankton and bacteria lipids, indicating particle disaggregation and a deepwater ecosystem response. Predicted climate-induced increases in hurricane frequency and/or intensity may significantly alter ocean biogeochemical cycles by increasing the strength of the biological pump.

Plain Language Summary Hurricanes (tropical cyclones and typhoons) generate intense cooling and vertical mixing in the upper ocean, resulting in nutrient upwelling into the “sunlit” zone which fuels short-lived phytoplankton blooms. However, hurricanes' influence on the deep ocean remains unknown. Here we present direct evidence that hurricanes impact the ocean's “biological pump” by increasing export of labile (fresh and bioavailable) organic materials from the surface to the deep ocean. In October 2016, Hurricane Nicole tracked through the NW Atlantic Ocean passing near Bermuda. At 1,500 and 3,200 m depths, sinking particle fluxes of lipid compounds diagnostic of fresh, surface-derived phytoplankton detritus and zooplankton and microbial biomass increased by over an order of magnitude relative to lipid fluxes prior to Nicole. We also observed that suspended particles were highly enriched in these labile compounds, down to 1,700 m depth. Hurricane enhancement of the labile carbon flux is important as this flux supports deep ocean ecosystems, affects ocean cycling of nutrients and other bioreactive elements, and regulates deep ocean oxygen consumption. The sensitivity of the ocean carbon cycle to extreme weather events furthermore suggests that climate-induced changes in hurricane frequency and intensity will impact the ocean's biological pump and deep ocean ecosystems.

1. Introduction

Tropical cyclones (hurricanes) are the most extreme episodic weather event affecting the subtropical and temperate ocean. Hurricanes generate strong near-inertial waves and mixing impact air-sea heat and carbon dioxide fluxes (Bates et al., 1998; Black & Dickey, 2008; Brink, 1989; Price, 1981; Price et al., 2008; Zhang et al., 2016). Surface mixed layer deepening and upwelling generated by Ekman pumping during hurricane passage upwells nutrients into the euphotic zone which induces transient phytoplankton blooms, visible by satellite (Babin et al., 2004; Foltz et al., 2015; Lin et al., 2003; Platt et al., 2005; Son et al., 2006). While the influence of hurricanes on surface ocean physics and biogeochemistry is now relatively well understood, the impact of hurricanes on the ocean's biological pump and deep ocean environment remains essentially unknown.

Since 1850, over 100 hurricanes passing through the North Atlantic subtropical gyre have tracked within 300 km of Bermuda (Figure 1a). On 13 October 2016, Hurricane Nicole, a Category 3 hurricane with a 136 km radius of hurricane-force winds, passed through the Bermuda Time Series site, the location of several ongoing multidecadal ocean time series: Hydrostation S time series of hydrographic parameters (Michaels & Knap, 1996; Phillips & Joyce, 2007; Steinberg et al., 2001), the Bermuda Atlantic Time series Study

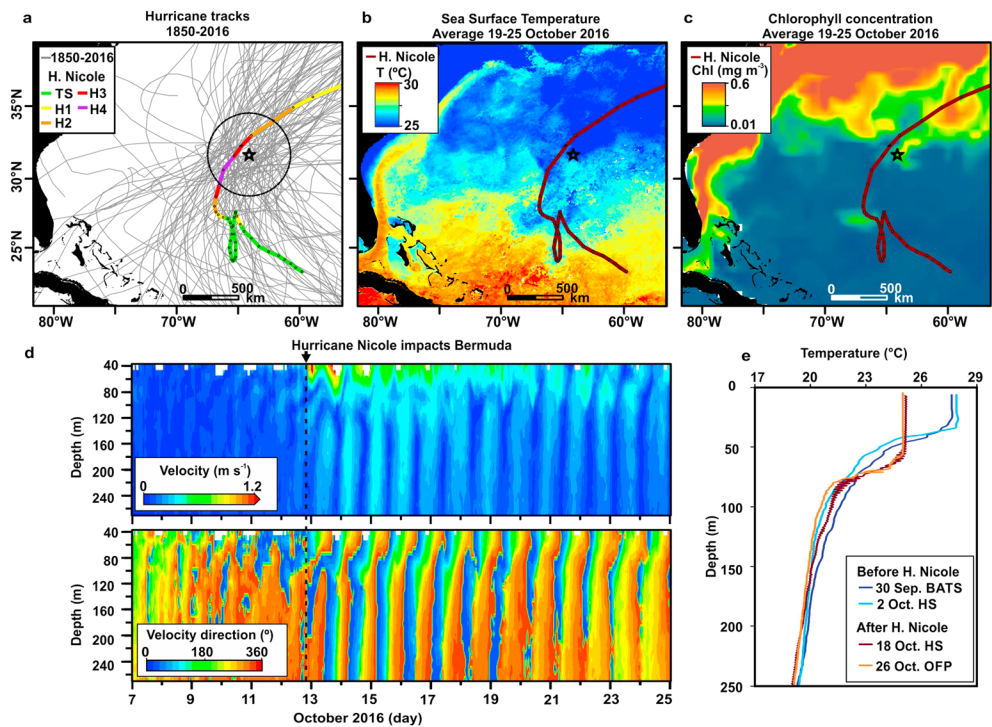


Figure 1. Hurricane activity near Bermuda. (a) Hurricanes passing within 300 km (black circle) of the Bermuda Time Series Site (black star) from 1850 to 2016. The Hurricane Nicole track is color coded with Saffir-Simpson Wind Scale: TS (tropical storm) and hurricane (H, Categories 1–4). Nicole's closest approach was 13 October 2016, with 56 m s⁻¹ maximum sustained winds and a 136 km hurricane-force wind radius. (b, c) Weekly averaged sea surface temperature and chlorophyll concentration, respectively, following Nicole's passage over Bermuda. (d) Current magnitude (m s⁻¹) and direction (°) before, during, and after passage of Hurricane Nicole. (e) Temperature profiles before (blue lines) and after (red and orange lines) passage of Hurricane Nicole at the BATS, HS, and OFP sites. BATS = Bermuda Atlantic Time series Study; HS = Hydrostation S; OFP = Oceanic Flux Program.

(BATS) time series of upper ocean biogeochemistry (Lomas et al., 2013; Michaels & Knap, 1996; Steinberg et al., 2001), and the Oceanic Flux Program (OFP) time series of deep ocean fluxes (Conte et al., 2001; Conte & Weber, 2014).

The timing of Nicole's passage provided a unique opportunity to directly assess the impacts of the hurricane on surface ocean biogeochemistry and the biological pump. In this study, we synthesize multidisciplinary data from hydrographic and phytoplankton measurements and lipid compositional data of sinking and suspended particles collected over the Nicole event to evaluate the impact of hurricanes on the ocean's biological pump and carbon export to the deep ocean.

2. Material and Methods

2.1. Hydrographic and Remote Sensing data

The description and relative locations of the Bermuda time series are provided in Text S1 and Figure S1 in the supporting information. Measurements of oceanographic conditions before and after Hurricane Nicole were collected on Hydrostation S, BATS, and OFP cruises. Temperature profiles were measured on Conductivity, Temperature, and Depth (CTD) casts.

Current profiles in the upper 280 m of the water column were continuously measured over the study period by the upward looking 150-KHz Acoustic Doppler Current Profiler (RDI/Teledyne Quarter Master) that is affixed to the top of the OFP mooring (300 m depth).

Sea surface temperature (SST) data (8-day SST composites) were obtained from Moderate Resolution Imaging Spectrometer, in orbit on the Aqua platform, using 4-km resolution Level 3 binned data. Eight-

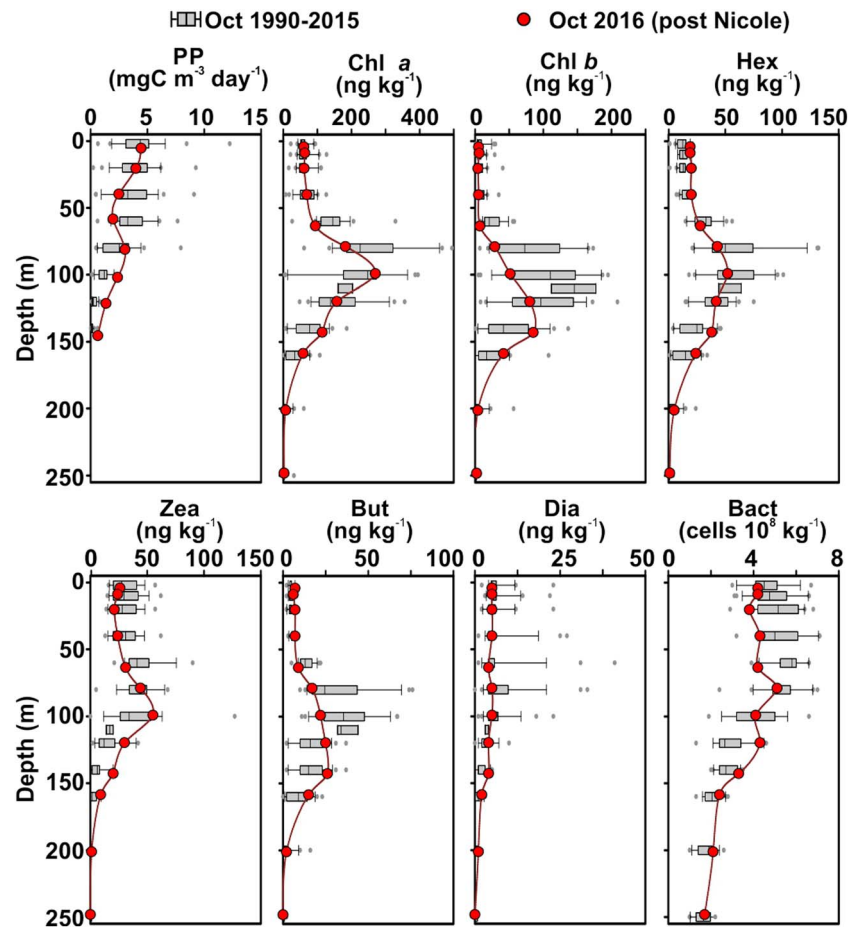


Figure 2. Phytoplankton response to Hurricane Nicole. Box-whisker plots (gray) of primary production (PP) and pigment and bacteria concentrations in the upper 250 m during October from 1990 to 2016 (n ranges from 13 to 24 due to sampling variability). The box shows the 25th percentile and 75th percentile quartiles and the median, bars show the 5% and 95% data distribution, and circles show the outliers. Profiles 5 days after Nicole are shown by red circles. Pigment abbreviations and taxonomic significance (Aiken et al., 2009): Chlorophyll *a*, (Chl *a*, photosynthetic algal pigment), Chlorophyll *b* (Chl *b*, Chlorophytes), 19-Hexanoyloxyfucoxanthin (Hex, Haptophytes), Zeaxanthin (Zea, Cyanobacteria), 19-Butanoyloxyfucoxanthin (But, Chrysophytes), Diadinoxanthin (Dia, diatoms, Haptophytes), and bacteria abundance (Bact).

day mean SST data are processed and distributed by the National Aeronautics and Space Administration Goddard Earth Sciences Data, Information Services Center, and Ocean Biology Processing Group. Seven-day mean surface Chl concentration data were obtained from Pelagic Interaction Scheme for Carbon and Ecosystem Studies (HAMOCC v.5, Aumont et al., 2015).

Hurricane position and intensity information were obtained from the National Oceanic and Atmospheric Administration National Hurricane Center (see Text S2).

2.2. Sample Collection

Water samples for bacteria cell counts and phytoplankton pigment concentrations were collected from Niskin bottles on CTD casts conducted on 19 October 2016 (6 days after Hurricane Nicole's passage and 7 days before the suspended particle collection). Sinking particles were collected at 1,500 and 3,200 m depths by Parflux sediment traps (McLane Labs, Falmouth, MA) on the OFP mooring. Trap cups were filled with 40-ppt deep seawater (concentrated by freezing) poisoned with ultratrace metal purity HgCl_2 (200 mg L^{-1}). OFP methods are detailed in Conte et al. (2001, 2018). Sinking particles analyzed in this study were collected between 25 October 2016 and 10 December 2016 with a biweekly sample resolution. Suspended particle collection and analyses are detailed in Pedrosa-Pàmies et al. (2018) and Text S2.

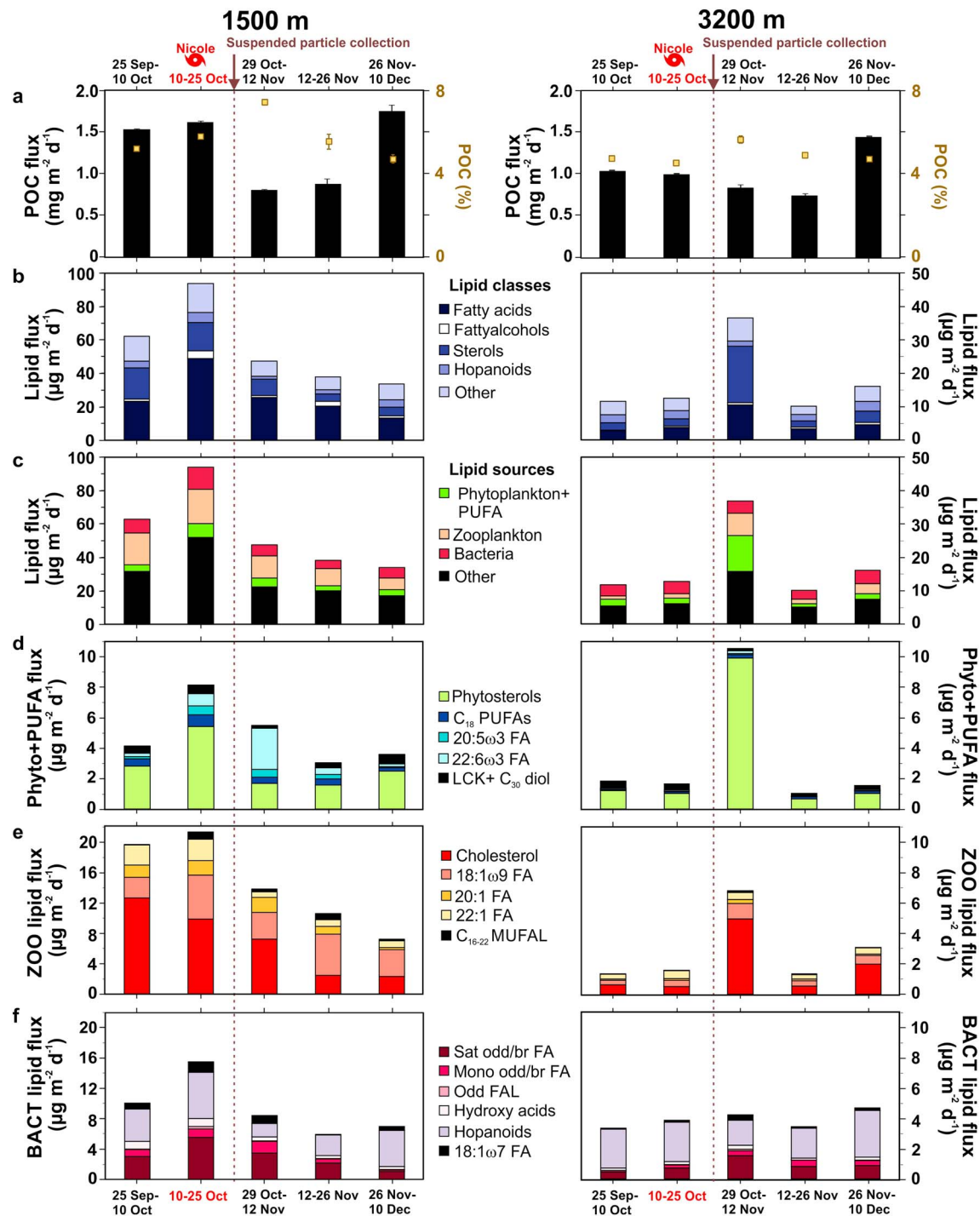


Figure 3. Lipid fluxes at 1,500 and 3,200 m depths before, during, and after Nicole. (a) Particulate organic carbon (POC) flux and percentage of the total mass flux (yellow). (b) Total lipid flux with contributions of fatty acids (FA), fatty alcohols (FAL), and sterols and nonspecific lipids (Other). (c) Fluxes of POC sourced from phytoplankton-derived and labile material (Phytoplankton+PUFA), Zooplankton, Bacteria, and Other (see text). Fluxes of diagnostic lipid biomarkers for (d) phytoplankton-derived POC (Phyto+PUFA): phytosterols (Table S1), long-chain alkenones (LCK) and C_{30} diols, and PUFA compounds (C_{18} PUFAs, $20:5\omega3$, and $22:6\omega3$). (e) Zooplankton-derived POC (ZOO): cholesterol, $18:1\omega9$, $20:1\omega9$, $22:1\omega9$, and $22:1\omega11$ monounsaturated fatty acids (MUFA); and C_{16-22} monounsaturated fatty alcohols (MUFAL). (f) Bacteria-derived POC (BACT): odd and branched fatty acids (odd/br FA), $18:1\omega7$ MUFA, odd FAL, hydroxy acids, and hopanoids (HOP).

2.3. Analytical Methods

Analytical methods for phytoplankton production, pigments, and bacterial cell enumeration used methods described in the BATS Methods Manual (Knap et al., 1997) and are detailed in Text S2.

Particulate organic carbon (POC) concentrations were measured on a Europa 20-20 CF-IRMS interfaced with a Europa ANCA-SL elemental analyzer. Samples were acidified prior to analysis to remove carbonates (Text S2). Analytical uncertainty was $<0.07\%$ ($n \geq 3$).

Lipids were preserved and analyzed using a modification of methods in Conte et al. (2003) (Pedrosa-Pàmies et al., 2018) and described in Text S2. Briefly, an internal standard mixture (n -C_{21:0} fatty alcohol, n -C_{23:0} fatty acid, 5 α (H)-cholestane, and n -C_{36:0} alkane) was added to the samples prior to lipid extraction. Lipids were ultrasonically extracted in 2:1 CHCl₃-MeOH, transesterified with methanolic HCl and trimethylsilylated using BSTFA with 1% TMCS. The transesterified, trimethylsilyl derivatives were analyzed on an Agilent 7890A GC coupled to a 5975C MS equipped with triple-axis MS and FID detectors. Compounds were identified by mass spectra and quantified from their FID response relative to the internal standard. Uncertainties in quantification range between 4% and 11%, based upon repeated analyses of samples having similar lipid composition.

Over a hundred extractable lipid compounds are present in oceanic POC. Current knowledge of taxonomic distributions and diagenetic transformations allows inferences in sources and lability (i.e., “lability/freshness” or ease of degradability). We estimated the relative contributions of POC sources by summing the absolute and POC-normalized concentrations of key lipid biomarkers into groups: Phytoplankton-derived POC and labile polyunsaturated fatty acids (PHYTO+PUFA), zooplankton-derived POC (ZOO), and bacterial-derived POC (BACT; see Figure 3 and Tables S1 and S2 for abbreviation details)

1. PHYTO+PUFA = C₁₈ FA + 20:5 ω 3 FA + 22:6 ω 3 FA + phytosterols + alkenones + C₃₀ diol
2. ZOO = 18:1 ω 9 FA + 20:1 ω 9 MUFA + 22:1 ω 9 MUFA + 22:1 ω 11 MUFA + cholesterol + MUFAL
3. BACT = Odd/br FA + 18:1 ω 7 FA + odd FAL + hopanoids + hydroxy acids

2.4. Multivariate Analysis

Principal component analysis (PCA) was performed to assess compositional variation of sinking and suspended particles. PCA used a total of 49 POC-normalized observations and included 16 key lipid biomarkers as variables (section 2.3). The observations include five sinking particle samples for each 1,500 and 3,200 m depths, collected before, during, and after Hurricane Nicole and 39 observations of suspended particles collected in October 2016 two weeks following passage of Hurricane Nicole, in April 2015 (postspring bloom conditions) and November 2015 (minimum production conditions; see Pedrosa-Pàmies et al., 2018 for further details).

3. Results and Discussion

3.1. Upper Ocean Physical and Biological Response to Hurricane Nicole

Nicole became a tropical storm on 4 October 2016 and circled the tropical Atlantic for 6 days before accelerating and intensifying as it approached the Bermuda Time Series Site. Closest approach was on 13 October. Remote sensing of SST and chlorophyll following Nicole's passage showed a typical pattern of surface ocean cooling (Babin et al., 2004; Foltz et al., 2015; Lin et al., 2003) and evidence of induced phytoplankton blooms (Figures 1b–1c and S2).

Current profiles (Figure 1d) showed that Nicole generated strong currents (up to 1 ms⁻¹ at 80 m depth) that persisted for over 2 days and near-inertial waves that persisted for over 2 weeks. The mixed layer deepened by 25 m and cooled by 2.9 °C in response to the hurricane physical forcing (Figure 1e). These observations are similar to those previously observed for other hurricanes passing through the Bermuda region (Black & Dickey, 2008; Dickey et al., 1998; Goni et al., 2017; Price, 1981).

Depth profiles of primary production rates, phytoplankton pigment, and bacteria cell concentrations were measured 6 days after Nicole (Figure 2). These profiles showed enhancement and deepening of primary production, phytoplankton pigments, and bacteria cell concentrations relative to that typically observed in October. Primary production rates and pigment and bacteria concentrations below the euphotic zone (typically ~100 m depth; Siegel et al., 2001) were among the highest observed in October over the last 25 years of

BATS sampling. These observations indicated that Nicole induced a transient phytoplankton bloom that was subsequently downmixed into subeuphotic zone waters. Similar responses were observed at the BATS site following Hurricanes Felix (Category 1, August 1995) and Fabian (Category 3, September 2003; Figure S3). These observations are consistent with other evidence for nutrient stimulation of phytoplankton production, particularly diatoms (Maiti et al., 2009; Malone et al., 1993; Marra et al., 1990), following extreme wind events in the Sargasso Sea (Malone et al., 1993; Marra et al., 1990) and in the NE Atlantic Ocean (Painter et al., 2016), NW Pacific Ocean China Sea (Chung et al., 2012), and coastal regions (Anglès et al., 2015; Gauns et al., 2016).

3.2. Deep Ocean Particle Flux and Composition Following Hurricane Nicole

The deep particle flux was continuously sampled by the OFP traps as Nicole passed through the region (Figure 3). At 1,500 m, while the total POC flux did not increase during Nicole's passage, the POC percentage of the flux increased by 30% (29 October to 12 November). The total lipid flux increased by 34%, from $60 \mu\text{g}\cdot\text{m}^{-2}\cdot\text{day}^{-1}$ (4.1% of POC) to $94 \mu\text{g}\cdot\text{m}^{-2}\cdot\text{day}^{-1}$ (5.8% of POC) in the period sampled during Nicole's passage (10–25 October). Subsequently, the lipid flux declined by 50% and continued to decline over the rest of November and December. Fluxes of phytoplankton-derived lipids (phytosterols, C_{18} PUFAs, and the C_{30} diols) increased by up to 100% during Nicole, indicating rapid delivery of phytodetritus to the deep ocean after the overlying bloom (Figures 3c and 3d and Table S1). The doubling of fluxes of phytosterols prevalent in diatoms (Volkman, 2003; $\text{nor}C_{27}\Delta^{5,22}$, $C_{27}\Delta^{5,22}$, and $C_{28}\Delta^{5,22}$) suggests that diatoms contributed a sizable portion of the phytodetritus flux, even though pigment composition (Figure 2) indicated that diatoms were relatively minor components of phytoplankton biomass. Fluxes of zooplankton-derived lipids (18:1 ω 9 fatty acid and C_{16-22} monounsaturated fatty alcohols) also increased twofold and eightfold, respectively, concurrent with the increase in phytodetritus flux. Similarly, fluxes of bacteria-derived lipids (18:1 ω 7 fatty acid, odd- and branched-chained fatty acids, and hopanoids) increased by 40–80%. Fluxes of steroidal ketones, early degradation products of sterols, increased by 20% and fluxes of 1-O-alkylglycerols, presumed to be sourced from both animals and bacteria, increased by a remarkable 270% (Table S1).

Flux composition at 1,500 m depth evolved over the Nicole event (Figure 4). POC-normalized concentrations of phytosterols and bacterial hopanoids were highest during the period of highest lipid flux, while concentrations of C_{20-22} PUFA and most zooplankton- and other bacteria-derived biomarkers were highest after the peak in lipid flux (Figures 3 and 4 and Table S1). These observations suggest continued reworking of the labile carbon flux materials by animal and microbial activities.

A clear time lag was observed in the arrival of the phytodetrital flux at 3,200 m depth. Total lipid flux increased threefold from 10–25 October to 29 October to 12 November, from $13 \mu\text{g}\cdot\text{m}^{-2}\cdot\text{day}^{-1}$ (1.3% of POC) to $37 \mu\text{g}\cdot\text{m}^{-2}\cdot\text{day}^{-1}$ (4.4% of POC; Figures 3a–3c). As observed at 1,500 m depth, the POC percentage of the mass flux increased by 27%, coincident with the increase in lipid flux, after Nicole's passage. The lipid flux peak was particularly enriched in phytosterols and steroidal ketones, which increased by an order of magnitude (Table S1). Similarly, fluxes of zooplankton-derived cholesterol and 18:1 ω 9 fatty acid increased by 100% and 70%, respectively, and fluxes of bacteria-derived odd- and branched-chained fatty acids and alcohols increased by 100%. POC-normalized concentrations of phytosterols were highest during the period of the maximum lipid flux (Figure 4). Similar trends were observed for most zooplankton- and bacteria-derived biomarkers and indicates a continuing close coupling of heterotrophic biomass and activity with the labile phytodetritus flux, even at bathypelagic depths (Figures 3 and 4).

Large amorphous aggregates were observed in both the 1,500 and 3,200 m flux material during the period of maximum fluxes (Figure S5). This formation of rapidly sinking particles by physical (coagulation) and/or biological (animal ingestion) particle aggregation of phytoplankton and other materials accelerated the transfer of bloom-derived materials to the deep ocean.

3.3. Surface Export and Deep Ocean Response to Hurricane Nicole's Passage

The increase in labile lipid export following Hurricane Nicole's passage is reflected in the elevated lipid concentrations observed in suspended particles within mesopelagic waters 2 weeks after Nicole's passage (Figure S4; Pedrosa-Pàmies et al., 2018). The enrichment in fresh, labile organic carbon in lower mesopelagic waters is particularly noteworthy for phytoplankton-derived compounds (e.g., phytosterols, C_{30} diol, and alkenones) and for rapidly degraded PUFA.

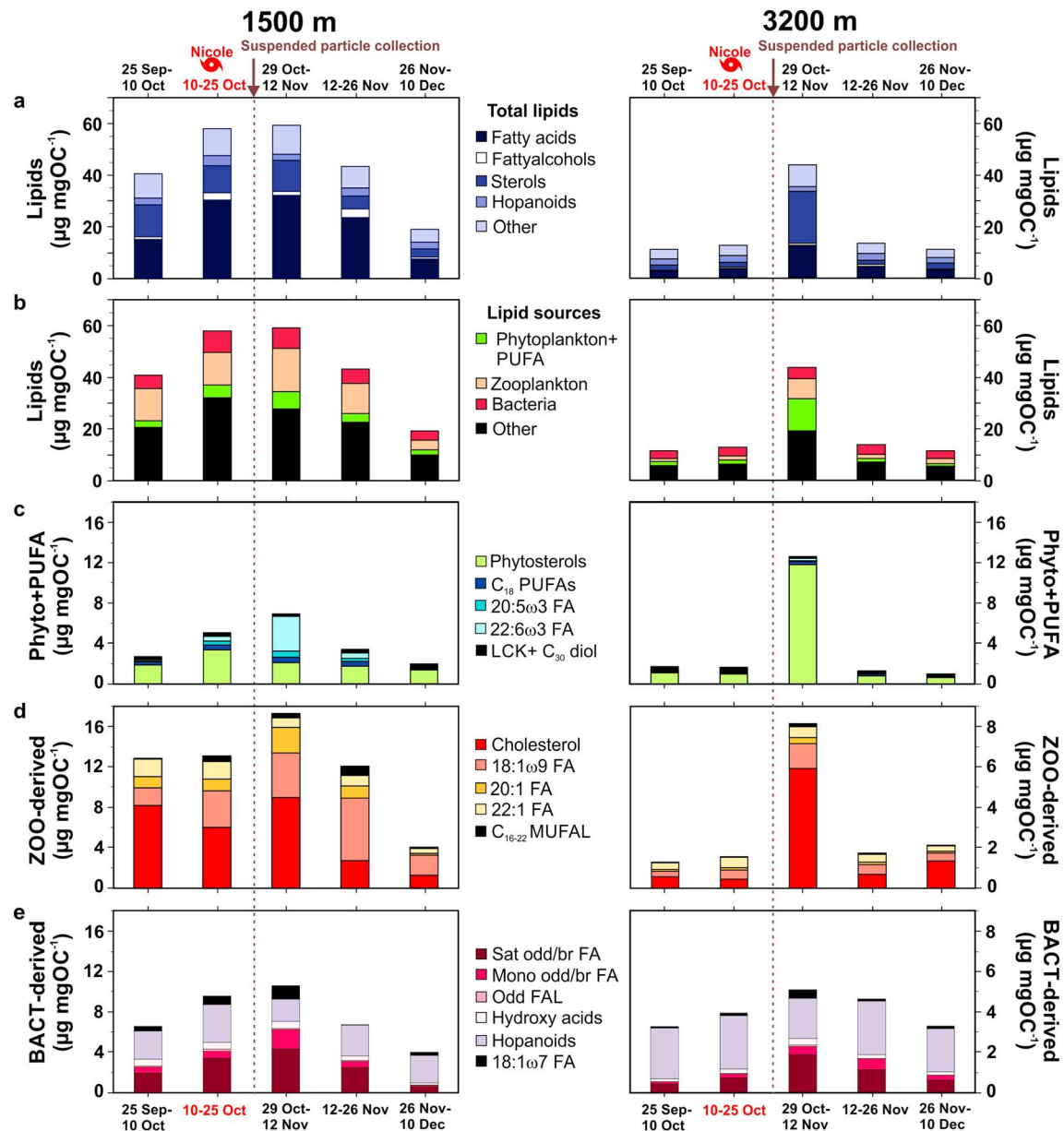


Figure 4. POC-normalized lipid concentrations in the particle flux at 1,500 and 3,200 m depths before, during, and after Nicole's passage. (a) Total lipid flux. (b) Concentrations sourced from phytoplankton-derived and labile material (Phytoplankton+PUFA), zooplankton-derived, bacteria-derived, and Other. Concentrations of diagnostic lipid biomarkers of (c) phytoplankton-derived POC (Phyto+PUFA), (d) zooplankton-derived POC (ZOO), and (e) bacteria-derived POC (BACT). (See Figure 3).

PCA was employed to quantitatively assess compositional changes. Results (Figures 5a and 5b) show high loadings on PC1 for compounds associated with phytoplankton-derived POC, PC2 for compounds associated with bacterial and zooplankton biomass, and PC3 for compounds associated with zooplankton biomass. Following Nicole, PC1 and PC3 factor scores for sinking particles increased at both 1,500 and 3,200 m depths (Figures 5c and 5d). Additionally, scores for suspended particles in mesopelagic waters after Nicole are significantly higher than in suspended particles during low productivity (November 2015) and postspring bloom (April 2015) conditions. These results highlight rapid export and disaggregation of surface bloom-derived material and an increase in animal- and bacteria-derived biomass in mesopelagic particles following Nicole. While part of the increase in zooplankton- and bacterial-derived lipids in the

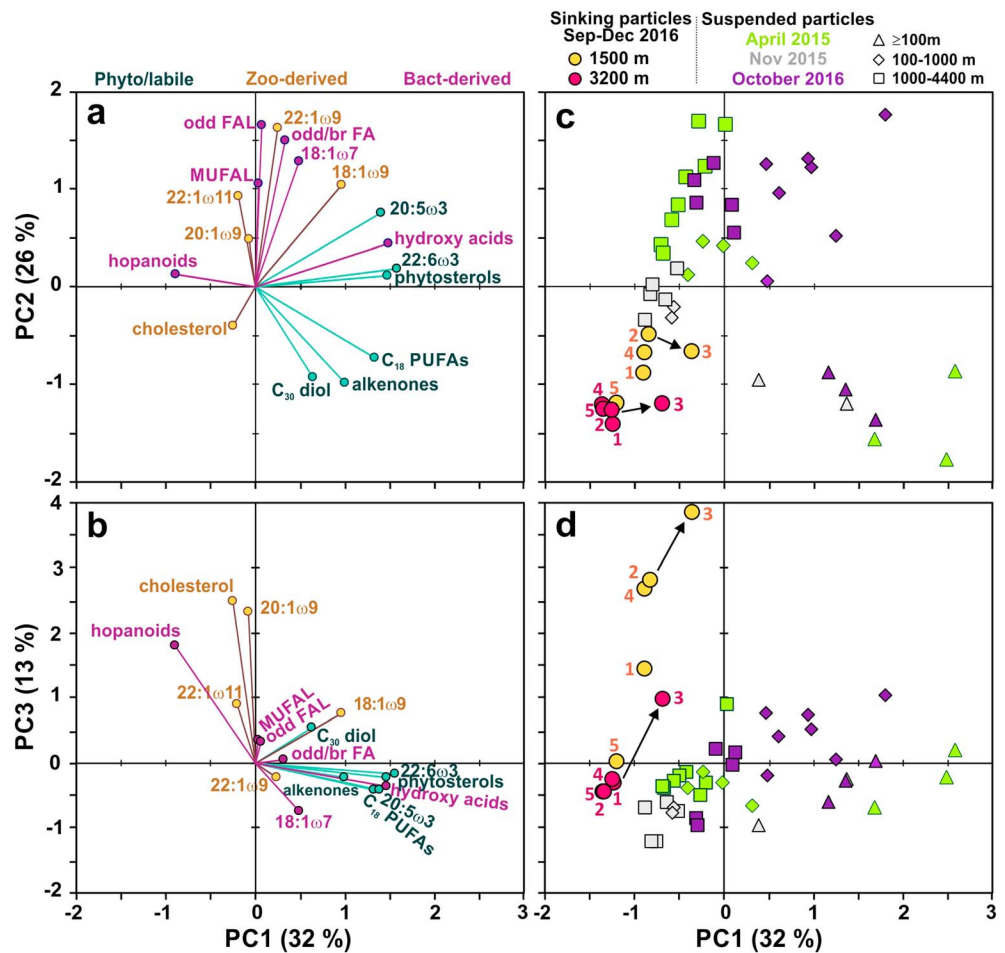


Figure 5. PCA results. (a, b) Factor loadings for biomarkers of phytoplankton/labile material (PHYTO+PUFA, green), zooplankton-derived material (ZOO, orange), and bacteria-derived material (BACT, purple). (c, d) Biplots of main factor scores for sinking and suspended particles, identified by depth zone. Sinking particles at 1,500 m (orange circles) and 3,200 m (pink circles) were collected during (1) 25 September to 10 October, (2) 10–25 October, (3) 29 October to 12 November, (4) 12–26 November, and (5) 26 November to 10 December. Suspended particle profiles were collected in April 2015 (green, post spring bloom conditions), November 2015 (gray, minimum production conditions), and in October 2016 two weeks after Nicole (purple). Black arrows indicate the increase in PC1 and PC3 scores following Nicole.

sinking and suspended particles was likely heterotrophic biomass directly associated with the sinking phytodetritus, lipid compositional changes in sinking particles (e.g., higher concentrations of cholesterol and hopanoids) and suspended particles (Pedrosa-Pàmies et al., 2018) evidence intensified particle recycling and deepwater secondary production in response to the arrival of labile carbon at depth.

4. Conclusions

This study shows, for the first time, that upper ocean physical perturbations associated with hurricane passage can enhance the export of labile carbon to the deep ocean and invoke a mesopelagic ecosystem response. The magnitude of the increases in total lipid and phytoplankton-derived lipid fluxes following Nicole is of the same magnitude as the increases in labile lipid fluxes that have been observed at 3,200 m depth at the Bermuda Time Series Site following mesoscale physical forcing of a transient bloom (Conte et al., 1998, 2003; Table S1). Previous studies have demonstrated that mesoscale ocean features can stimulate production and carbon export to the deep ocean (Conte et al., 2003; Pedrosa-Pàmies et al., 2016; Shih et al., 2015; Stukel et al., 2017), but the only prior documented evidence of storm-induced export of POC to depth is

the study of Chen et al. (2013) in the oligotrophic northwest Pacific Ocean, where an increase in flux of POC at 125 m depth was observed following an extreme weather event.

Seven hurricanes of Category 3 or greater have passed within 300 km of Bermuda between 1980 and 2016: Harvey 1981, Gert 1999, Erin 2001, Fabian 2003, Ophelia 2011, Gonzalo 2014, and Nicole 2016. Given the average radius of hurricane-force winds of ~135 km (Bell et al., 2004) for major hurricanes (Text S2), these hurricanes have affected an area of ~85,700 km² for the 36-year period, corresponding to an average surface area of ~23,000 km²/year (Figure S6).

The extensive area affected by hurricanes in subtropical and temperate regions suggests that hurricane forcing may significantly influence the biological pump and the efficiency of labile organic carbon export from the surface to the deep ocean. This in turn will impact the food supply for deep sea organisms (Gooday, 2002), microbial remineralization and oxygen consumption rates in the ocean interior (Baltar et al., 2016; Bochdansky et al., 2010; Herndl & Reinthaler, 2013), and the cycling of nutrients and easily remineralized, bioreactive elements (Conte et al., 2018; Weber et al., 2016).

The global impact of hurricane activity on the ocean carbon cycle remains to be evaluated. Although there are uncertainties in historical trends of hurricane intensity (Klotzbach et al., 2015; Sobel et al., 2016; Walsh et al., 2016; Yan et al., 2017), recent modeling studies suggest that hurricane intensity will increase as climate warms (Bhatia et al., 2019; Bianucci et al., 2018; Kossin, 2017). Further studies, in particular at long time series sites, are needed to elucidate the various effects of hurricanes on the oligotrophic ocean's biological pump. However, results here clearly indicate that climate-induced changes in hurricane frequency, intensity, and tracks may impact biogeochemical cycles, underscoring the sensitivity of the deep ocean and its ecosystems to climate perturbations (Kwon et al., 2009; Lima et al., 2014; Smith et al., 2013).

Acknowledgments

This work and the Oceanic Flux Program time series were supported by the National Science Foundation Chemical Oceanography Program Grant OCE 1536644. The Bermuda Atlantic Time Series and Hydrostation S time series were supported by NSF Grants OCE 1756105 and OCE 1633125, respectively. We acknowledge the contributions of BATS technicians with CTD and pigment analyses. We sincerely thank the officers and crew of R/V Atlantic Explorer (Bermuda Institute of Ocean Sciences) for their expert assistance on the cruises. The data used in this study are listed in the figures, tables, and references, and are also available in the NSF's Biological and Chemical Oceanography Data Management Office (BCO-DMO, <https://doi.org/10.1575/1912/bco-dmo.775902.1>).

References

- Aiken, J., Pradhan, Y., Barlow, R., Lavender, S., Poulton, A., & Hardman-Mountford, N. (2009). Phytoplankton pigments and functional types in the Atlantic Ocean: A decadal assessment, 1995–2005. *Deep Sea Research Part II: Topical Studies in Oceanography*, 56(15), 899–917. <https://doi.org/10.1016/J.DSR2.2008.09.017>
- Anglès, S., Jordi, A., & Campbell, L. (2015). Responses of the coastal phytoplankton community to tropical cyclones revealed by high-frequency imaging flow cytometry. *Limnology and Oceanography*, 60(5), 1562–1576. <https://doi.org/10.1002/lno.10117>
- Aumont, O., Ethé, C., Tagliabue, A., Bopp, L., & Gehlen, M. (2015). PISCES-v2: An ocean biogeochemical model for carbon and ecosystem studies. *Geoscientific Model Development*, 8(8), 2465–2513. <https://doi.org/10.5194/gmd-8-2465-2015>
- Babin, S. M., Carton, J. A., Dickey, T. D., & Wiggert, J. D. (2004). Satellite evidence of hurricane-induced phytoplankton blooms in an oceanic desert. *Journal of Geophysical Research*, 109, C03043. <https://doi.org/10.1029/2003JC001938>
- Baltar, F., Lundin, D., Palovaara, J., Lekunberri, I., Reinthaler, T., Herndl, G. J., & Pinhassi, J. (2016). Prokaryotic responses to ammonium and organic carbon reveal alternative CO₂ fixation pathways and importance of alkaline phosphatase in the mesopelagic North Atlantic. *Frontiers in Microbiology*, 7, 1670. <https://doi.org/10.3389/fmicb.2016.01670>
- Bates, N. R., Knap, A. H., & Michaels, A. F. (1998). Contribution of hurricanes to local and global estimates of air-sea exchange of CO₂. *Nature*, 395(6697), 58–61. <https://doi.org/10.1038/25703>
- Bell, K., Ray, P. S., Bell, K., & Ray, P. S. (2004). North Atlantic hurricanes 1977–99: Surface hurricane-force wind radii. *Monthly Weather Review*, 132(5), 1167–1189. [https://doi.org/10.1175/1520-0493\(2004\)132<1167:NAHSHW>2.0.CO;2](https://doi.org/10.1175/1520-0493(2004)132<1167:NAHSHW>2.0.CO;2)
- Bhatia, K. T., Vecchi, G. A., Knutson, T. R., Murakami, H., Kossin, J., Dixon, K. W., & Whitlock, C. E. (2019). Recent increases in tropical cyclone intensification rates. *Nature Communications*, 10(1), 635. <https://doi.org/10.1038/s41467-019-08471-z>
- Bianucci, L., Balaguru, K., Smith, R. W., Leung, L. R., & Moriarty, J. M. (2018). Contribution of hurricane-induced sediment resuspension to coastal oxygen dynamics. *Scientific Reports*, 8(1), 15740. <https://doi.org/10.1038/s41598-018-33640-3>
- Black, W. J., & Dickey, T. D. (2008). Observations and analyses of upper ocean responses to tropical storms and hurricanes in the vicinity of Bermuda. *Journal of Geophysical Research*, 113, C08009. <https://doi.org/10.1029/2007JC004358>
- Bochdansky, A. B., van Aken, H. M., & Herndl, G. J. (2010). Role of macroscopic particles in deep-sea oxygen consumption. *Proceedings of the National Academy of Sciences of the United States of America*, 107(18), 8287–8291. <https://doi.org/10.1073/pnas.0913744107>
- Brink, K. H. (1989). Observations of the response of thermocline currents to a hurricane. *Journal of Physical Oceanography*, 19(7), 1017–1022. [https://doi.org/10.1175/1520-0485\(1989\)019<1017:OOTROT>2.0.CO;2](https://doi.org/10.1175/1520-0485(1989)019<1017:OOTROT>2.0.CO;2)
- Chen, K.-S., Hung, C.-C., Gong, G.-C., Chou, W.-C., Chung, C.-C., Shih, Y.-Y., & Wang, C.-C. (2013). Enhanced POC export in the oligotrophic northwest Pacific Ocean after extreme weather events. *Geophysical Research Letters*, 40, 5728–5734. <https://doi.org/10.1002/2013GL058300>
- Chung, C., Gong, G., & Hung, C. (2012). Effect of Typhoon Morakot on microphytoplankton population dynamics in the subtropical Northwest Pacific. *Marine Ecology Progress Series*, 448, 39–49. <https://doi.org/10.3354/meps09490>
- Conte, M. H., Carter, A. M., Koweeck, D. A., Huang, S., & Weber, J. C. (2018). The elemental composition of the deep particle flux in the Sargasso Sea. *Chemical Geology*, 511, 279–313. <https://doi.org/10.1016/J.CHEMGEO.2018.11.001>
- Conte, M. H., Dickey, T. D., Weber, J. C., Johnson, R. J., & Knap, A. H. (2003). Transient physical forcing of pulsed export of bioreactive material to the deep Sargasso Sea. *Deep Sea Research Part I: Oceanographic Research Papers*, 50(10–11), 1157–1187. [https://doi.org/10.1016/S0967-0637\(03\)00141-9](https://doi.org/10.1016/S0967-0637(03)00141-9)
- Conte, M. H., & Weber, J. (2014). Particle flux in the deep Sargasso Sea: The 35-year oceanic flux program time series. *Oceanography*, 27(1), 142–147. <https://doi.org/10.5670/oceanog.2014.17>

- Conte, M. H., Weber, J. C., King, L. L., & Wakeham, S. G. (2001). The alkenone temperature signal in western North Atlantic surface waters. *Geochimica et Cosmochimica Acta*, 65(23), 4275–4287. [https://doi.org/10.1016/S0016-7037\(01\)00718-9](https://doi.org/10.1016/S0016-7037(01)00718-9)
- Conte, M. H., Weber, J. C., & Ralph, N. (1998). Episodic particle flux in the deep Sargasso Sea. *Deep Sea Research Part I: Oceanographic Research Papers*, 45(11), 1819–1841. [https://doi.org/10.1016/S0967-0637\(98\)00046-6](https://doi.org/10.1016/S0967-0637(98)00046-6)
- Dickey, T., Frye, D., McNeil, J., Manov, D., Nelson, N., Sigurdson, D., et al. (1998). Upper-ocean temperature response to Hurricane Felix as measured by the Bermuda testbed mooring. *Monthly Weather Review*, 126(5), 1195–1201. [https://doi.org/10.1175/1520-0493\(1998\)126<1195:UOTRTH>2.0.CO;2](https://doi.org/10.1175/1520-0493(1998)126<1195:UOTRTH>2.0.CO;2)
- Foltz, G. R., Balaguru, K., & Leung, L. R. (2015). A reassessment of the integrated impact of tropical cyclones on surface chlorophyll in the western subtropical North Atlantic. *Geophysical Research Letters*, 42, 1158–1164. <https://doi.org/10.1002/2015GL063222>
- Gauns, M., Kurian, S., Shenoy, D. M., Naik, H., & Naqvi, S. W. A. (2016). Cyclone phytoplankton community succession in the coastal waters off Goa, India. *Current Science*, 111(6), 1091–1097. <https://doi.org/10.18520/cs/v111/i6/1091-1097>
- Goni, G., Todd, R., Jayne, S., Halliwell, G., Glenn, S., Dong, J., et al. (2017). Autonomous and Lagrangian ocean observations for Atlantic tropical cyclone studies and forecasts. *Oceanography*, 30(2), 92–103. <https://doi.org/10.5670/oceanog.2017.227>
- Gooday, A. J. (2002). Biological responses to seasonally varying fluxes of organic matter to the ocean floor: A review. *Journal of Oceanography*, 58(2), 305–332. <https://doi.org/10.1023/A:1015865826379>
- Herdnl, G. J., & Reinthaler, T. (2013). Microbial control of the dark end of the biological pump. *Nature Geoscience*, 6(9), 718–724. <https://doi.org/10.1038/ngeo1921>
- Klotzbach, P. J., Landsea, C. W., Klotzbach, P. J., & Landsea, C. W. (2015). Extremely intense hurricanes: Revisiting Webster et al. (2005) after 10 Years. *Journal of Climate*, 28(19), 7621–7629. <https://doi.org/10.1175/JCLI-D-15-0188.1>
- Knap, A. H., Michaels, A. F., Steinberg, D. K., Bahr, F., Bates, N. R., Bell, S., Countway, P., Close, A. R., Doyle, A. P., Dow, R. L., Howse, F. A., Gundersen, K., Johnson, R. J., Kelly, R., Little, R., Orcutt, K., Parsons, R., Rathburn, C., Sanderson, M., & Stone, S. (1997). BATS Methods Manual, Version 4. Woods Hole, MA, US: U.S. JGOFS Planning Office. Retrieved from <https://eprints.soton.ac.uk/361194/>
- Kossin, J. P. (2017). Hurricane intensification along United States coast suppressed during active hurricane periods. *Nature*, 541(7637), 390–393. <https://doi.org/10.1038/nature20783>
- Kwon, E. Y., Primeau, F., & Sarmiento, J. L. (2009). The impact of remineralization depth on the air–sea carbon balance. *Nature Geoscience*, 2(9), 630–635. <https://doi.org/10.1038/ngeo612>
- Lima, I. D., Lam, P. J., & Doney, S. C. (2014). Dynamics of particulate organic carbon flux in a global ocean model. *Biogeosciences*, 11(4), 1177–1198. <https://doi.org/10.5194/bg-11-1177-2014>
- Lin, I., Liu, W. T., Wu, C.-C., Wong, G. T. F., Hu, C., Chen, Z., et al. (2003). New evidence for enhanced ocean primary production triggered by tropical cyclone. *Geophysical Research Letters*, 30(13), 1718. <https://doi.org/10.1029/2003GL017141>
- Lomas, M. W., Bates, N. R., Johnson, R. J., Knap, A. H., Steinberg, D. K., & Carlson, C. A. (2013). Two decades and counting: 24-years of sustained open ocean biogeochemical measurements in the Sargasso Sea. *Deep Sea Research Part II: Topical Studies in Oceanography*, 93, 16–32. <https://doi.org/10.1016/J.DSR2.2013.01.008>
- Maiti, K., Benitez-Nelson, C. R., Lomas, M. W., & Krause, J. W. (2009). Biogeochemical responses to late-winter storms in the Sargasso Sea, III—Estimates of export production using ^{234}Th : ^{238}U disequilibria and sediment traps. *Deep Sea Research Part I: Oceanographic Research Papers*, 56(6), 875–891. <https://doi.org/10.1016/J.DSR.2009.01.008>
- Malone, T. C., Pike, S. E., & Conley, D. J. (1993). Transient variations in phytoplankton productivity at the JGOFS Bermuda time series station. *Deep Sea Research Part I: Oceanographic Research Papers*, 40(5), 903–924. [https://doi.org/10.1016/0967-0637\(93\)90080-M](https://doi.org/10.1016/0967-0637(93)90080-M)
- Marra, J., Bidigare, R. R., & Dickey, T. D. (1990). Nutrients and mixing, chlorophyll and phytoplankton growth. *Deep Sea Research Part A: Oceanographic Research Papers*, 37(1), 127–143. [https://doi.org/10.1016/0198-0149\(90\)90032-Q](https://doi.org/10.1016/0198-0149(90)90032-Q)
- Michaels, A. F., & Knap, A. H. (1996). Overview of the U.S. JGOFS Bermuda Atlantic Time-series Study and the Hydrostation S program. *Deep Sea Research Part II: Topical Studies in Oceanography*, 43(2–3), 157–198. [https://doi.org/10.1016/0967-0645\(96\)00004-5](https://doi.org/10.1016/0967-0645(96)00004-5)
- Painter, S. C., Finlay, M., Hemsley, V. S., & Martin, A. P. (2016). Seasonality, phytoplankton succession and the biogeochemical impacts of an autumn storm in the northeast Atlantic Ocean. *Progress in Oceanography*, 142, 72–104. <https://doi.org/10.1016/J.POCEAN.2016.02.001>
- Pedrosa-Pàmies, R., Conte, M. H., Weber, J. C., & Johnson, R. (2018). Carbon cycling in the Sargasso Sea water column: Insights from lipid biomarkers in suspended particles. *Progress in Oceanography*, 168, 248–278. <https://doi.org/10.1016/J.POCEAN.2018.08.005>
- Pedrosa-Pàmies, R., Sanchez-Vidal, A., Canals, M., Lampadariou, N., Velaoras, D., Gogou, A., et al. (2016). Enhanced carbon export to the abyssal depths driven by atmosphere dynamics. *Geophysical Research Letters*, 43, 8626–8636. <https://doi.org/10.1002/2016GL069781>
- Phillips, H. E., & Joyce, T. M. (2007). Bermuda's tale of two time series: Hydrostation S and BATS. *Journal of Physical Oceanography*, 37(3), 554–571. <https://doi.org/10.1175/JPO2997.1>
- Platt, T., Bouman, H., Devred, E., Fuentes-Yaco, C., Sathyendranath, S., & Sathyendranath, S. (2005). Physical forcing and phytoplankton distributions. *Scientia Marina*, 69(S1), 55–73. <https://doi.org/10.3989/scimar.2005.69s155>
- Price, J. F. (1981). Upper ocean response to a hurricane. *Journal of Physical Oceanography*, 11(2), 153–175. [https://doi.org/10.1175/1520-0485\(1981\)011<0153:UORTAH>2.0.CO;2](https://doi.org/10.1175/1520-0485(1981)011<0153:UORTAH>2.0.CO;2)
- Price, J. F., Morzel, J., & Niiler, P. P. (2008). Warming of SST in the cool wake of a moving hurricane. *Journal of Geophysical Research*, 113, C07010. <https://doi.org/10.1029/2007JC004393>
- Shih, Y.-Y., Hung, C.-C., Gong, G.-C., Chung, W.-C., Wang, Y.-H., Lee, I.-H., et al. (2015). Enhanced particulate organic carbon export at eddy edges in the oligotrophic western north Pacific Ocean. *PLoS One*, 10(7), e0131538. <https://doi.org/10.1371/journal.pone.0131538>
- Siegel, D. A., Westberry, T. K., O'Brien, M. C., Nelson, N. B., Michaels, A. F., Morrison, J. R., et al. (2001). Bio-optical modeling of primary production on regional scales: The Bermuda BioOptics project. *Deep Sea Research Part II: Topical Studies in Oceanography*, 48(8–9), 1865–1896. [https://doi.org/10.1016/S0967-0645\(00\)00167-3](https://doi.org/10.1016/S0967-0645(00)00167-3)
- Smith, K. L., Ruhl, H. A., Kahru, M., Huffard, C. L., & Sherman, A. D. (2013). Deep ocean communities impacted by changing climate over 24 y in the abyssal northeast Pacific Ocean. *Proceedings of the National Academy of Sciences of the United States of America*, 110(49), 19,838–19,841. <https://doi.org/10.1073/pnas.1315447110>
- Sobel, A. H., Camargo, S. J., Hall, T. M., Lee, C.-Y., Tippet, M. K., & Wing, A. A. (2016). Human influence on tropical cyclone intensity. *Science*, 353(6296), 242–246. <https://doi.org/10.1126/SCIENCE.AAF6574>
- Son, S., Platt, T., Bouman, H., Lee, D., & Sathyendranath, S. (2006). Satellite observation of chlorophyll and nutrients increase induced by Typhoon Megi in the Japan/East Sea. *Geophysical Research Letters*, 33, L05607. <https://doi.org/10.1029/2005GL025065>

- Steinberg, D. K., Carlson, C. A., Bates, N. R., Johnson, R. J., Michaels, A. F., & Knap, A. H. (2001). Overview of the US JGOFS Bermuda Atlantic Time-series Study (BATS): A decade-scale look at ocean biology and biogeochemistry. *Deep Sea Research Part II: Topical Studies in Oceanography*, *48*(8–9), 1405–1447. [https://doi.org/10.1016/S0967-0645\(00\)00148-X](https://doi.org/10.1016/S0967-0645(00)00148-X)
- Stukel, M. R., Aluwihare, L. I., Barbeau, K. A., Chekalyuk, A. M., Goericke, R., Miller, A. J., et al. (2017). Mesoscale ocean fronts enhance carbon export due to gravitational sinking and subduction. *Proceedings of the National Academy of Sciences of the United States of America*, *114*(6), 1252–1257. <https://doi.org/10.1073/pnas.1609435114>
- Volkman, J. K. (2003). Sterols in microorganisms. *Applied Microbiology and Biotechnology*, *60*(5), 495–506. <https://doi.org/10.1007/s00253-002-1172-8>
- Walsh, K. J. E., McBride, J. L., Klotzbach, P. J., Balachandran, S., Camargo, S. J., Holland, G., et al. (2016). Tropical cyclones and climate change. *Wiley Interdisciplinary Reviews: Climate Change*, *7*(1), 65–89. <https://doi.org/10.1002/wcc.371>
- Weber, T., Cram, J. A., Leung, S. W., DeVries, T., & Deutsch, C. (2016). Deep ocean nutrients imply large latitudinal variation in particle transfer efficiency. *Proceedings of the National Academy of Sciences*, *113*(31), 8606–8611. <https://doi.org/10.1073/pnas.1604414113>
- Yan, X., Zhang, R., & Knutson, T. R. (2017). The role of Atlantic overturning circulation in the recent decline of Atlantic major hurricane frequency. *Nature Communications*, *8*(1), 1695. <https://doi.org/10.1038/s41467-017-01377-8>
- Zhang, H., Chen, D., Zhou, L., Liu, X., Ding, T., & Zhou, B. (2016). Upper ocean response to typhoon Kalmaegi (2014). *Journal of Geophysical Research: Oceans*, *121*, 6520–6535. <https://doi.org/10.1002/2016JC012064>